doi:10.1017/S1431927622001696
Microsc. Microanal. 28 (Suppl 1), 2022

Advanced Crack Analytics on 3D X-ray Tomography of Irradiated Silicon Carbide Claddings

Fei Xu[1*], Joshua J. Kane[1], Peng Xu[1], Nikolaus Cordes[1], Jason L. Schulthess[1], Mahmut Nedim Cinbiz[1], Sean Gonderman[2], Christian Deck[2] and Jack Gazza[2]

[1.] Idaho National Laboratory, Idaho Falls, ID, United States.
[2.] General Atomics, San Diego, CA, United States.
* Corresponding author: fei.xu@inl.gov

Silicon Carbide **(**SiC) ceramic matrix composite (CMC) cladding is currently being pursued as one of the leading candidates for accident tolerant fuels. One of the grand challenges is to determine the porosity and leak path, if any, non-destructively. Three-dimensional (3D) X-ray imaging, also referred to as X-ray computed tomography (CT), is a data-rich characterization technique that can provide surface and subsurface spatial information in a non-destructive manner. In this paper, we present the 3D X-ray tomography data coupled with novel analytic methods to unveil the defects in SiC CMC cladding for the first time.

Non-destructively 3D imaging was performed using ZEISS Xradia 520 Versa X-ray microscope (Carl Zeiss X-ray Microscopy Inc., Dublin, CA, USA) at INL's Materials and Fuels Complex. The Nordson DAGE tungsten X-ray source (Aylesbury, UK) was operated with a proprietary high energy filter, 110.9-kVp accelerating voltage, and 111.7-µA target current. All projection radiographs were acquired over 360 degrees of sample rotation, and each radiograph had an average of 20 image frames. The frame size is 3024 by 3064 pixels. Additional detail is listed in Table 1.

Table 1 3D X-ray data information of three samples

Sample	Source to the Rotation Axis (RA) (mm)	Detector to the RA (mm)	Pixel Size (µm)	Number of Projections	Cone Angle
1	-26.0461	245.4407	7.1762	4,501	14.9334
2	-26.0461	245.4392	7.1763	4,501	14.9040
3	-21.0601	234.2374	6.1704	2,401	15.8031

Conventional crack detection was only performed on the material surfaces, which was unable to directly evaluate the material performance since the cracks/voids/leak paths and structures under the material surfaces were invisible. Therefore, there is a pressing need to develop a fully automatic approach that accurately extracts the voids/cracks, visualize the void/crack connective structure, and potential leak paths.

In this paper, we developed a fully automatic workflow to detect and analyze cracks using image processing techniques on 3D X-ray images (Fig. 1). Void/crack detection, visualization, and analysis are the three major components, including four processing blocks, noted as P_1 to P_4. P_1 spatially aligned the cylindrical axis orthogonal to the volumetric Z-axis and extracted the smallest possible volume of interest within a Cartesian coordinate system. Since slices of 3D X-ray exist rotating and drifting during reconstruction, the material centers vary from different samples. We designed an automatic algorithm to extract the sub-image containing the material part. P_2 was applied to unwrap the material annular by transforming the volume from a Cartesian coordinate to polar coordinate system, which reduced the image size, and hence the computational burden, by nearly 60 times less. P_3 detected and labeled the voids/cracks using image segmentation approaches, including smoothing/enhancing the image before detection, applying global threshold to detect the voids, and removing the artifacts with post-processing. P_4 generated the connected structures of 3D visualized voids/cracks and statistical results. More experimental results of other samples are shown in Fig. 2.

The experimental results demonstrated that Sample 1 and Sample 2 have cracks establishing a continuous path between the interior and exterior surface of the annulus breaking the desired hermiticity of the material, and no such cracks were observed in Sample 3. These results demonstrate the applicability of X-ray tomographic imaging capability in rapidly supporting post-irradiation examinations of non-fuel components X-ray tomography with advanced visualization methods and automated defect analysis [1].

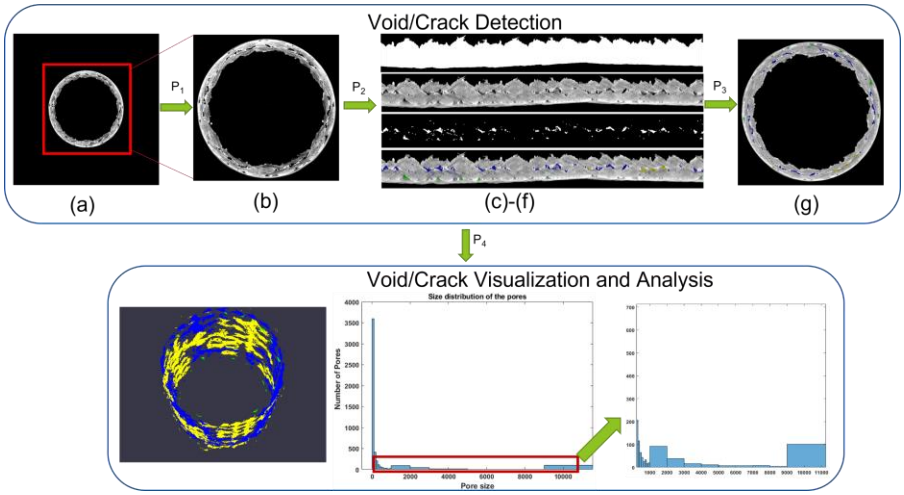

Figure 1. The proposed workflow. (a) An image from Sample 3 with field of view representing 3024×3064; (b) sub-image containing material annulus; (c)-(f) represent a spatially transformed coordinate system of Sample 3 showing from top to bottom a binary segmentation of the annulus, original grayscale reconstruction, segmented voids, and color-coded pore classifications. In (f):green denotes the voids/cracks connected directly to the outer surface of the annulus; blue identifies closed voids/cracks that do not touch the inner or outer surface of the annulus; yellow identifies voids/cracks touching the inner surface of the annulus; and red identifies voids/cracks touching the inner and outer surfaces. (g) Rewrapped image frame with corresponding classifications from (f).

https://doi.org/10.1017/S1431927622001696 Published online by Cambridge University Press

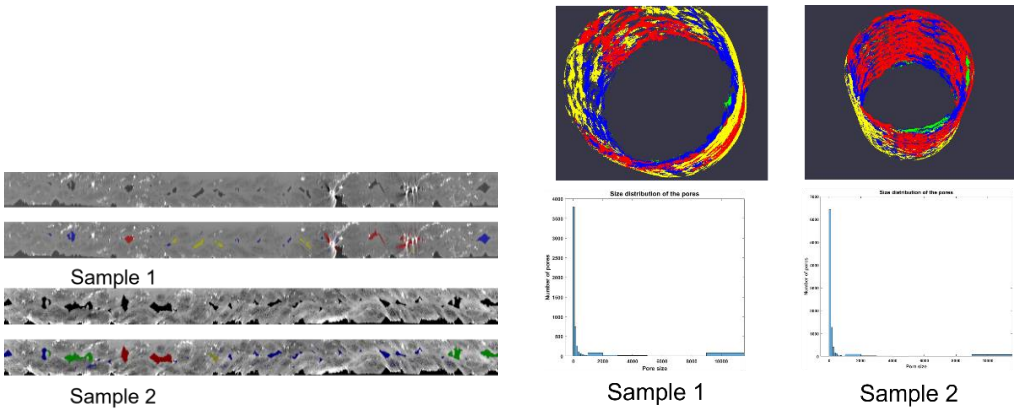

Figure 2 Experimental results on sample 1 and sample 2.

References:

[1] This research is being performed using funding received from Advanced Fuel Campaign and GA ATF CRADA (Cooperative Research and Development Agreement).

https://doi.org/10.1017/S1431927622001696 Published online by Cambridge University Press